

Optimization of an Offline Pulse-Shape Discrimination Technique for the Liquid Scintillator BC-501A

September 2006

Prepared by

**Marek Flaska
Sara A. Pozzi**

DOCUMENT AVAILABILITY

Reports produced after January 1, 1996, are generally available free via the U.S. Department of Energy (DOE) Information Bridge.

Web site <http://www.osti.gov/bridge>

Reports produced before January 1, 1996, may be purchased by members of the public from the following source.

National Technical Information Service
5285 Port Royal Road
Springfield, VA 22161
Telephone 703-605-6000 (1-800-553-6847)
TDD 703-487-4639
Fax 703-605-6900
E-mail info@ntis.gov
Web site <http://www.ntis.gov/support/ordernowabout.htm>

Reports are available to DOE employees, DOE contractors, Energy Technology Data Exchange (ETDE) representatives, and International Nuclear Information System (INIS) representatives from the following source.

Office of Scientific and Technical Information
P.O. Box 62
Oak Ridge, TN 37831
Telephone 865-576-8401
Fax 865-576-5728
E-mail reports@osti.gov
Web site <http://www.osti.gov/contact.html>

This report was prepared as an account of work sponsored by an agency of the United States Government. Neither the United States government nor any agency thereof, nor any of their employees, makes any warranty, express or implied, or assumes any legal liability or responsibility for the accuracy, completeness, or usefulness of any information, apparatus, product, or process disclosed, or represents that its use would not infringe privately owned rights. Reference herein to any specific commercial product, process, or service by trade name, trademark, manufacturer, or otherwise, does not necessarily constitute or imply its endorsement, recommendation, or favoring by the United States Government or any agency thereof. The views and opinions of authors expressed herein do not necessarily state or reflect those of the United States Government or any agency thereof.

Nuclear Science and Technology Division

**OPTIMIZATION OF AN OFFLINE PULSE-SHAPE DISCRIMINATION TECHNIQUE
FOR THE LIQUID SCINTILLATOR BC-501A**

Marek Flaska and Sara A. Pozzi

Date Published: September 2006

Prepared by
OAK RIDGE NATIONAL LABORATORY
P.O. Box 2008
Oak Ridge, Tennessee 37831-6285
managed by
UT-BATTELLE, LLC
for the
U.S. DEPARTMENT OF ENERGY
under contract DE-AC05-00OR22725

Contents

Figures	v
Abstract	vii
1. Introduction.....	1
2. Motivation.....	1
3. Identification Procedure for Neutron Sources	2
4. Proposed PSD Technique	3
4.1 Acquisition of Pulses.....	3
4.2 Description of the PSD Technique	4
4.3 The PSD Optimization	6
4.3.1 Optimization of the total integration limit	6
4.3.2 Optimization of the tail integration limit	7
4.3.3 Optimization of the location of classification point.....	8
4.3.4 Optimization of the pulse-height threshold	8
4.3.5 Application of the optimized PSD method to known neutron pulses.....	11
4.4 Application of the Optimized PSD Method to Unknown Pulses	12
5. Conclusions and Future Work	14
6. Acknowledgments.....	15
7. References.....	15

Figures

1.	Major procedure steps towards neutron source identification	2
2.	Neutron and gamma-ray pulses measured with liquid scintillation detector BC-501A	4
3.	Description of the ratio of the tail-to-total integral	4
4.	Typical histograms of neutron and gamma-ray pulses	5
5.	Curves created from the neutron and gamma-ray histograms shown in Fig. 4	6
6.	Total overlap area as a function of the starting point of the tail integral	7
7.	Histograms of neutron and gamma-ray pulses obtained by using the optimized range of the tail integral	8
8.	Total overlap area as a function of the ratio of the tail-to-total integral	9
9.	The tail integral versus the total integral from raw data	10
10.	The tail integral versus the total integral using the optimized pulse-shape discrimination method	10
11.	Comparison of pulse-height distributions created using known neutron pulses	11
12.	The measurement setup used to test the optimized pulse-shape discrimination method	12
13.	Histogram from unknown data	13
14.	Comparison of neutron pulse-height distributions; known versus unknown data	14

Abstract

This report describes a pulse-shape discrimination method that can be used to distinguish neutrons from gamma rays measured with liquid scintillation detectors. The proposed method is based on offline pulse analysis and allows discrimination of neutrons from gamma rays with an accuracy of 3% for time-of-flight attributed neutrons. A fast oscilloscope Tektronix TDS-5104 in combination with a liquid scintillation detector BC-501A was used to detect and store the neutron and gamma-ray pulses. The Matlab® scripts were written to post-process the data and to optimize the discrimination method. Because there is a difference in a slow component of the light produced by neutron and gamma rays, a specific ratio of tail-to-total integral is proposed for particle identification. The tail integration range and location of the classification point were optimized using “known” neutron and gamma-ray pulses to minimize the number of misclassified particles. This method can be further improved by increasing the detector pulse-height threshold.

1. Introduction

Accurate knowledge of the spectrum of neutrons emitted by nuclear materials is of great interest in many research applications, such as nuclear nonproliferation, international safeguards, nuclear material control and accountability, national security, and counterterrorism. Therefore it is very important to develop methods that allow fast and robust identification of neutron sources and unfolding of neutron spectra. For safeguards applications it is essential to correctly identify specific neutron sources such as Cf-252, americium-beryllium, or Pu-240. In addition, the possibility of performing an accurate unfolding of neutron spectra increases the sensitivity of assays performed on various nuclear materials [1].

Neutron and gamma-ray pulse-shape discrimination (PSD) using liquid scintillation detectors is a widely adopted technique in these fields [2]. Liquid scintillators are frequently used in nonproliferation applications due to their excellent neutron/gamma PSD properties. Most present neutron measurement devices use thermal neutron detectors, such as He-3 counters, to detect neutrons originating from fissile materials. However, because these detectors require thermalization of the neutrons before detection, all information relative to the neutron spectrum is lost. In contrast, liquid scintillators are able to detect high-energy neutrons and thus do not need to use moderating material. This important characteristic allows instruments that use liquid scintillators to provide a more accurate characterization of nuclear materials. For this reason, organic liquid scintillators are expected to become a main component of future portable measurement systems. Generally, the decision time of currently adopted PSD techniques lies in the range of hundreds of nanoseconds [3-5]. A shorter decision time would allow for higher count rates and thus further increase the sensitivity of the assays performed on nuclear materials and help achieve the main objective of detecting and determining the mass and composition of these materials.

2. Motivation

Neutron spectrum unfolding relies on the accurate identification of the pulse-height distribution generated by the neutron source in the radiation detector. Because liquid scintillators are sensitive to both neutrons and gamma rays, a robust and efficient pulse-shape discrimination technique is essential to determine the *neutron* pulse-height distribution accurately. Once this distribution has been determined, neutron unfolding techniques can be applied to obtain the initial neutron energy spectrum. The neutron spectrum represents a unique “signature” of a neutron source and can be used for source identification.

One complication in the unfolding procedures arises because small variations in measured pulse-height distributions lead to large variations in the unfolded neutron spectrums.

Because some of the gamma rays measured may be counted as neutrons, introducing further uncertainty, it is crucial to identify neutrons with a high degree of accuracy.

The goal of this report is to present a method of discriminating neutrons from gamma rays originating from an “unknown” source with high accuracy. This accurate discrimination is essential for any unfolding technique to obtain the incident neutron source spectrum and will

allow identification of neutron sources in a fast and robust way.

3. Identification Procedure for Neutron Sources

Fig. 1 is a flowchart illustrating the major steps of a proposed procedure to correctly identify various neutron sources.

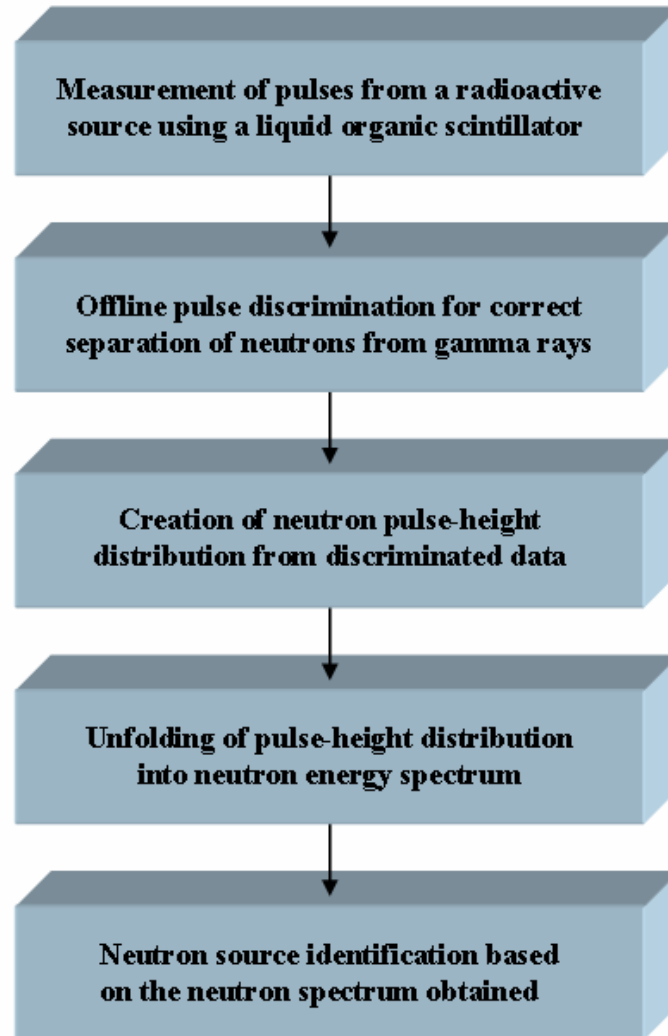


Fig. 1. Major steps in neutron source identification.

This report addresses the first three steps shown in Fig. 1. In particular, this document focuses on the description of an offline PSD technique. All results acquired by measurements were post-processed using the Matlab® software.

4. Proposed PSD Technique

4.1 Acquisition of Pulses

A fast waveform digitizer, phosphor oscilloscope Tektronix TDS-5104 with a 1-GHz resolution, was used to efficiently store tens of thousands of pulses from the anode of the liquid scintillator BC-501A for subsequent analysis. The oscilloscope fast-frame acquisition mode allowed us to capture the pulses with a high resolution. The BC-501A scintillation detector is well-known for its excellent neutron/gamma discrimination properties. It is built using a cylindrical liquid organic scintillator model 4.62MAB-1F3BC-501A/5 (manufactured by Bicron), which is 7.7-cm thick and has a diameter of 15.2 cm. The detector container is made of aluminum. The front face of the detector has a thickness of 2 mm. The side wall is composed of two layers: the external layer has a thickness of 2 mm, while the internal layer is approximately 0.5-mm thick. The photomultiplier tube is mounted on the back circular surface of the detector.

As a first step in the present work, neutrons and gamma rays from two different radioactive sources were measured [6]. The neutrons emitted by a Cf-252 source were detected using the time-of-flight method (TOF), which allowed us to specifically identify the neutron pulses (with the exception of accidental coincidences) in a gamma-ray background. The Cf-252 source was placed in the middle of an ionization chamber at a distance of 1 m from the detector. The ionization chamber served as a “start” detector to determine the time zero. The neutron pulses obtained with this method are named “TOF attributed neutrons” in the remainder of this report. The reason for this nomenclature is that it is possible that some of the pulses attributed to neutrons were created by gamma rays due to accidental coincidences.

The gamma-ray pulses were measured using a Cs-137 source placed on the face of the detector. These gamma-ray pulses are named “gamma rays” in the remainder of this report. In this way, two sets of pulse data were obtained for the optimization of the PSD technique.

The oscilloscope fast-frame acquisition mode was used to capture the pulses, with a resolution of 0.2 ns. The pulses were binned into 14 groups of increasing and equal pulse area, resulting in approximately 500 to 1000 pulses per area bin. The pulses were then averaged to obtain average waveforms both for TOF attributed neutrons and gamma rays. The comparison is shown in Fig. 2, where it can be seen that the shape of the average gamma-ray pulses does not change with the area. However, the shape of the average neutron pulses shows significant differences in the tail of the pulse for pulses of different areas.

Fig. 2 also shows that the average neutron pulses have a more pronounced tail. In fact, the total light output generated in the scintillator can be represented by the sum of the two exponential decays referred to as the fast and slow components of the scintillation process. The fraction of the total light observed in the slow component is a function of the type of particle inducing the scintillation. In general, heavier particles produce more “delayed” light [7]. Therefore, the tails of the average neutron pulses are consistently greater than the tails of the gamma-ray pulses. This difference in the intensity of slow neutron and gamma-ray components serves as a basis for the proposed PSD method.

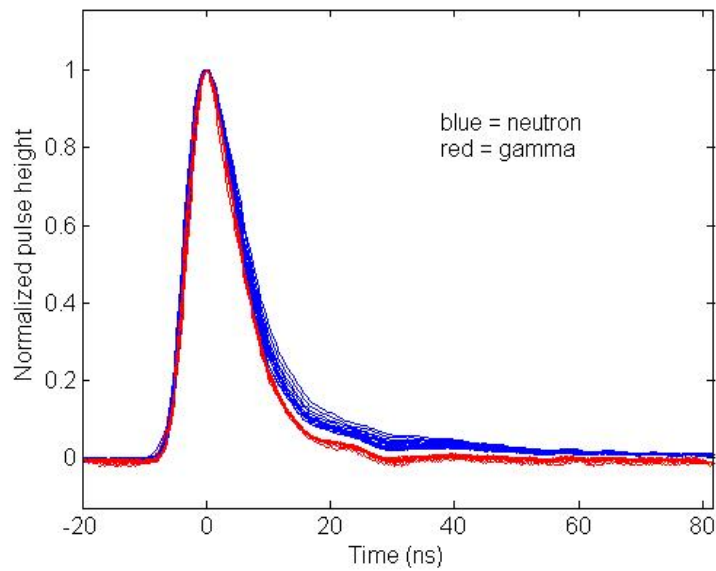


Fig. 2. Neutron and gamma-ray pulses measured with liquid scintillation detector BC-501A.

4.2 Description of the PSD Technique

On the basis of the observations in Sect. 4.1, we introduce a ratio of two areas obtained by integration of the pulse in various time intervals. The first area is the total area of the pulse (A_1), and the second area is the tail of the pulse (A_2). These areas are shown schematically in Fig. 3.

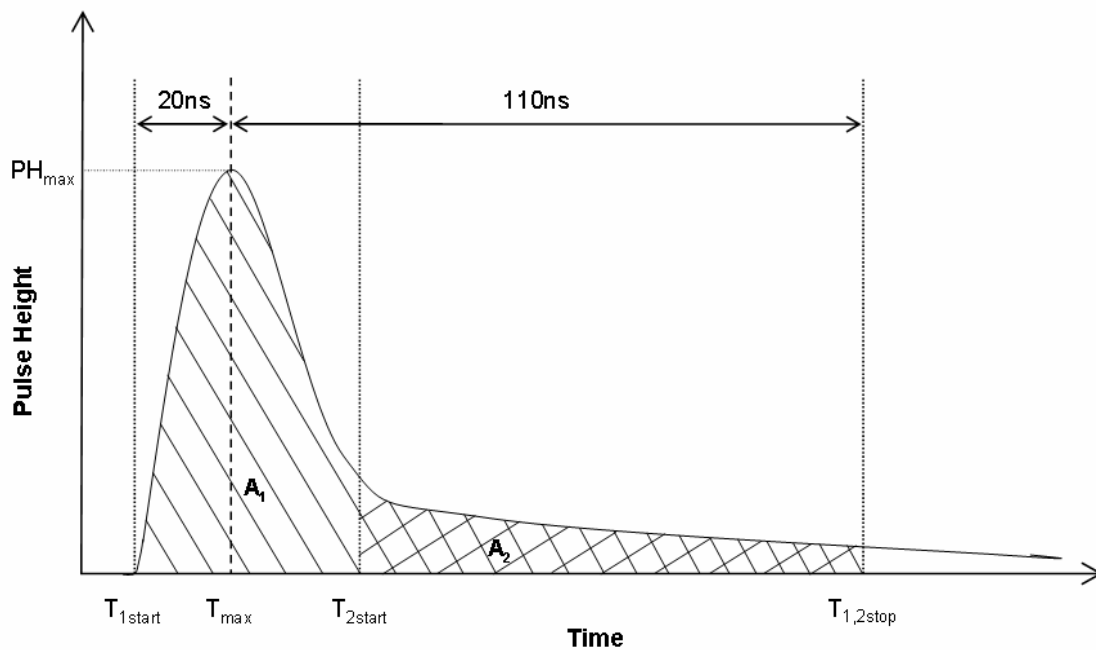


Fig. 3. Description of the ratio of the tail-to-total integral. The time scale of the measurement of “known” neutrons and gamma-ray pulses is also shown.

The area ratio is defined as

$$R = \frac{A_2}{A_1} . \quad (1)$$

As mentioned earlier, the intensity of the slow component in the light is higher for neutrons. Therefore neutron pulses have generally a higher ratio R . Fig. 4 shows an example of neutron and gamma-ray histograms in which the neutron and gamma-ray distributions can be clearly distinguished. The x-axis represents the ratio of the tail-to-total integral, while the y-axis shows the number of occurrences for a given R .

The tail integral A_2 is calculated from a certain point above the pulse maximum (see T_{2start} in Fig. 3) to the end of the pulse ($T_{1,2stop}$). In the case presented in Fig. 4, $T_{2start} = T_{max} + 6ns$, while $T_{1,2stop} - T_{max} = 110ns$. The latter is given by the time range used in our measurements and is valid for all results discussed later in this report. In contrast, the total integral A_1 is calculated by integrating between the values T_{1start} and $T_{1,2stop}$; thus it covers entire pulse areas ($T_{max} - T_{1start} = 20 ns$).

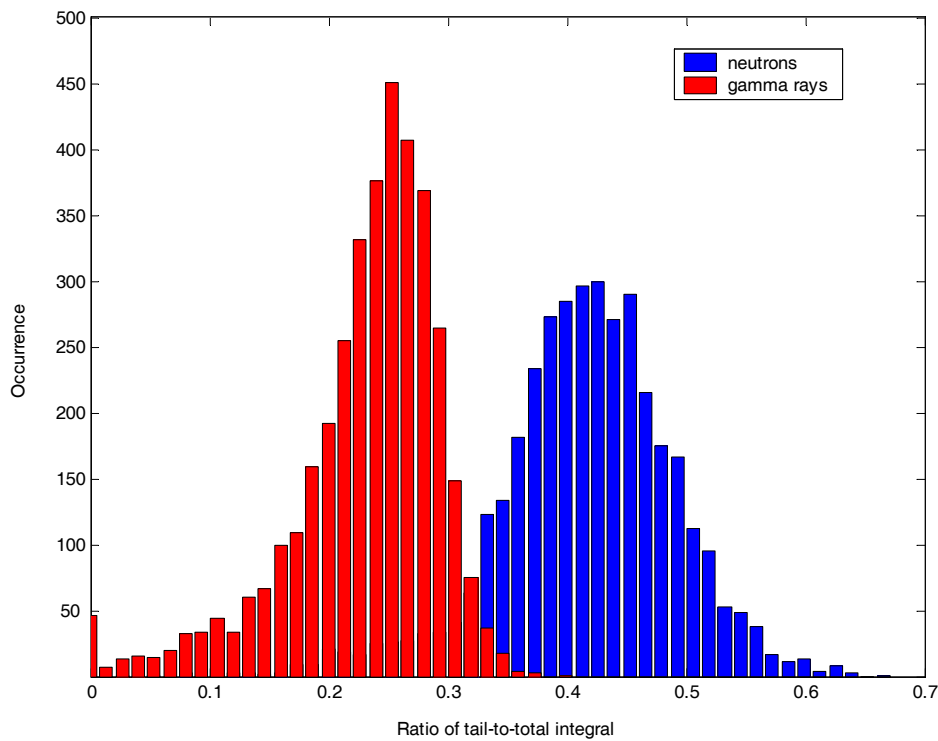


Fig. 4. Typical histograms of neutron and gamma-ray pulses. Two distributions can be clearly distinguished.

The integral ratio R is clearly higher for most of the neutron pulses when compared to the gamma-ray pulses. This feature can be used to separate the neutron pulses from the gamma rays. The relatively high value occurring in the gamma-ray histogram at position zero is due to the accumulation of low ratio values (negative ratio values are not possible). Fig. 5 shows the

distributions created from the histogram in Fig. 4. The cross point of the neutron and gamma curves has been chosen as a discrimination point to classify the particles detected. The point in this particular case lies at a value of 0.32. This value has not been optimized. Above the classification point all pulses are classified as neutrons, while below this point the pulses are classified as gamma rays. It can be seen in Fig. 5 that a certain number of neutrons and gamma rays are “misclassified” when using this technique. Therefore, optimization of this method is required, as described in Sect. 4.3.

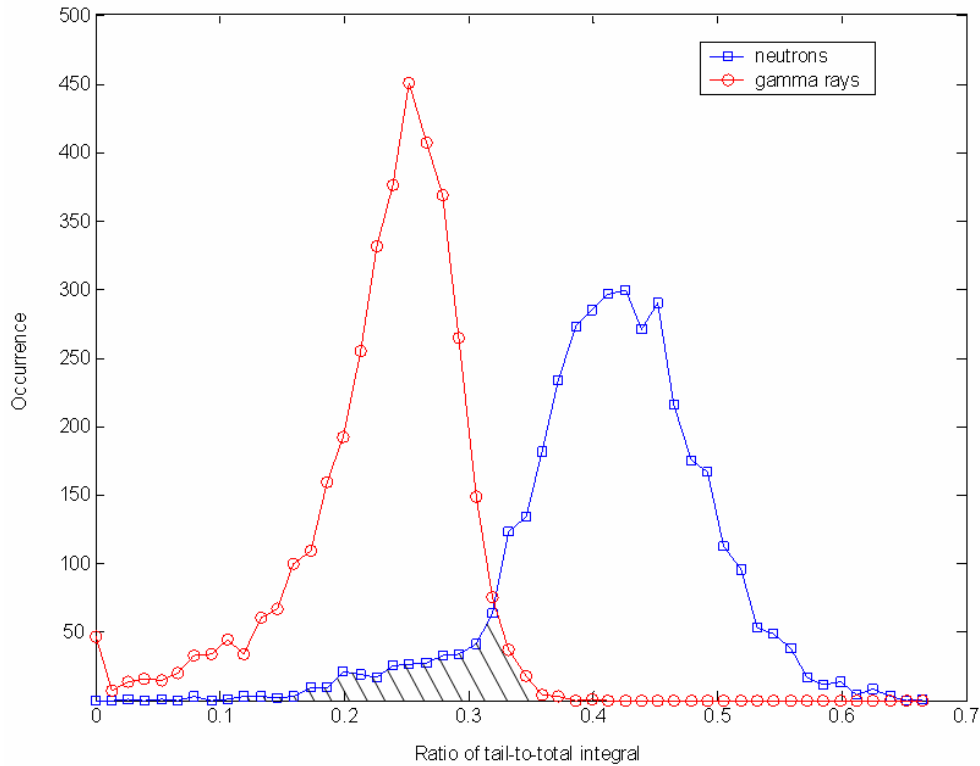


Fig. 5. Curves created from the neutron and gamma-ray histograms shown in Fig. 4. The “overlap area” is marked.

4.3 The PSD Optimization

The number of misclassified neutrons and gamma rays can be minimized by optimizing the following parameters: (1) the integration range of the total integral, (2) the integration range of the tail integral, (3) the location of the classification point, and (4) the pulse-height threshold. Optimizations (2) and (3) were applied to the problem and are discussed in the following sections in detail. Optimizations (1) and (4) will be discussed in detail in a future report.

4.3.1 Optimization of the total integration limit

Generally, the slow component of the light produced by the liquid scintillator BC-501A ends at approximately 300 ns [3]. However, in our measurements the pulse range was limited to 130 ns, which was given by the time scale chosen during the measurement. It is expected that an increase of the integration limit would lead to additional minimization of the overlap area. Therefore, the

Therefore, the influence of this parameter will be investigated in the future.

4.3.2 Optimization of the tail integration limit

Fig. 6 shows the overlap area as a function of the starting point of the tail integral A_2 . The upper limit for the tail integral was fixed to 110 ns. The x-axis in Fig. 6 is the time shift from the pulse maximum toward positive values (i.e., $T_{2\text{start}} - T_{\text{max}}$). As shown in Fig. 6, the overlap area reaches its minimum around 11 ns. At this point, the total overlap area reaches the minimum value of 3% from the total area of the neutron and gamma-ray distributions. For this reason, this value has been chosen as optimal for the tail integration. When using this value, the tail integral A_2 has a total range of 99 ns. The pulse-height threshold was set to 0.07 MeVee.

Fig. 7 shows the neutron and gamma-ray histograms obtained using the optimized tail integral. In Fig. 7 there is even higher occurrence in the gamma-ray histogram at position zero than that shown in Fig. 4. This is due to additional accumulation of low ratio values when compared to the situation presented in Fig. 4. This accumulation takes place as a result of shifting the neutron and gamma-ray histograms to lower values by shifting the starting point of the tail integral toward positive values. It is apparent that in this case the optimal classification point lies below 0.32, which is the value deduced from Fig. 5. The optimization of the classification point is discussed in the following section.

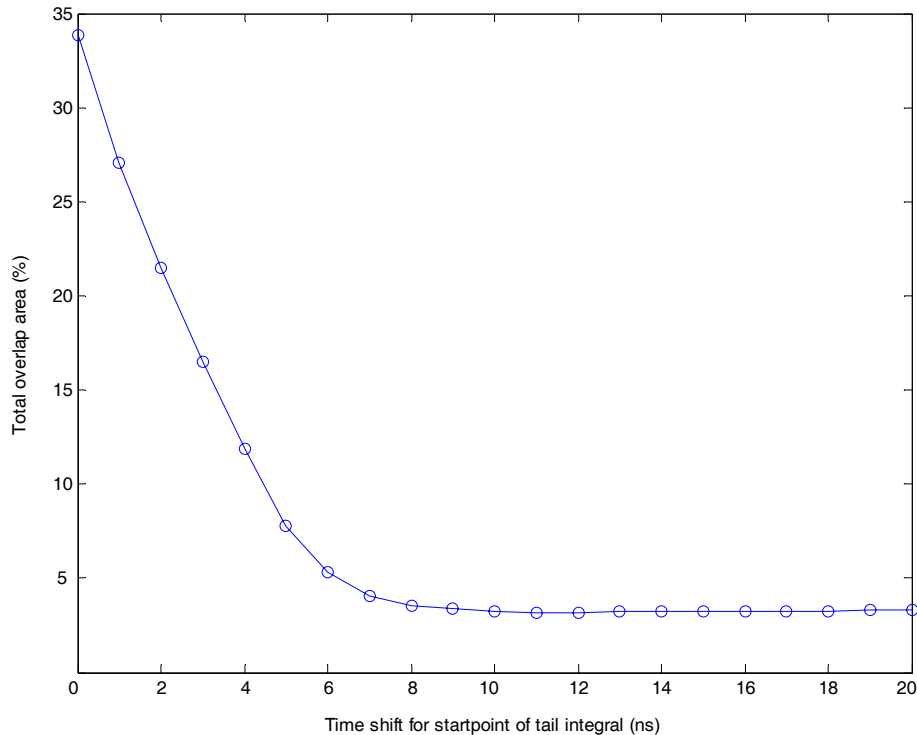


Fig. 6. Total overlap area as a function of the starting point of the tail integral. The x-axis is given by $T_{2\text{start}} - T_{\text{max}}$.

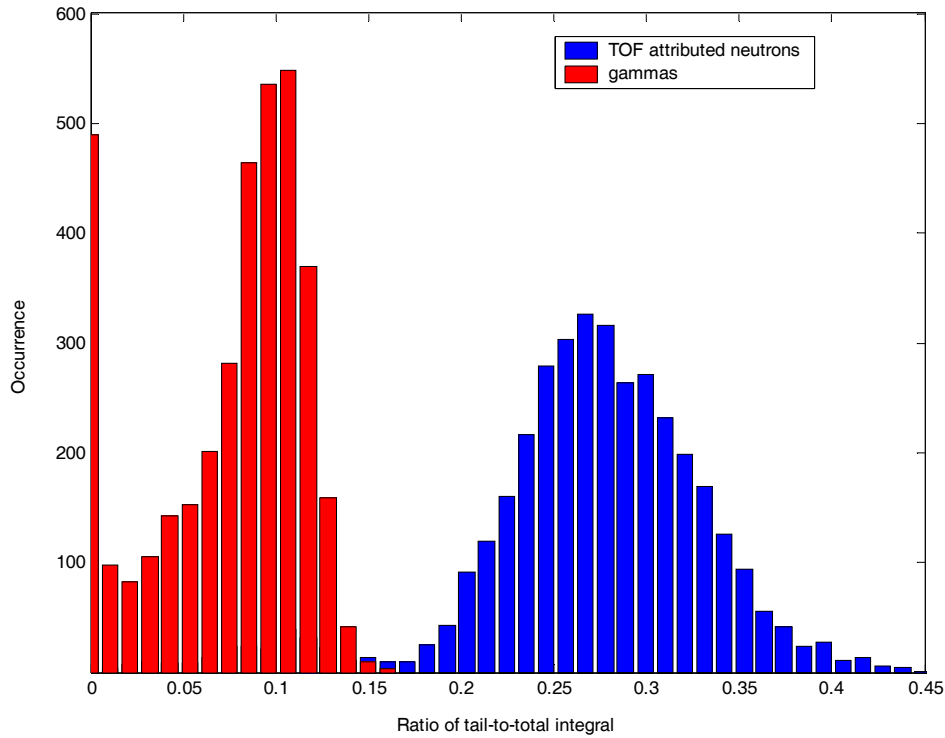


Fig. 7. Histograms of neutron and gamma-ray pulses obtained by using the optimized range of the tail integral.

4.3.3 Optimization of the location of classification point

Fig. 8 shows the number of misclassified neutrons and gamma rays as a function of the location of the classification point. As mentioned previously, all pulses (both neutron and gamma ray) are classified as neutrons when lying above this point, while those below this point are classified as gamma rays. Fig. 8 shows that this condition is fulfilled by choosing the classification point at a value of 0.15. At this point, approximately 3% of pulses are misclassified. Most of these pulses are neutrons, which means that almost no gamma rays are misclassified using the known pulses. The x-axis in Fig. 8 is identical to the one shown in Figs. 4 and 5. It should be noted that the classification point represents the central point at which the neutron and gamma-ray distributions overlap. Therefore it is also possible to estimate the classification point by observing the particle histogram (see Fig. 7).

4.3.4 Optimization of the pulse-height threshold

Another way of improving the PSD performance is to increase the value of the pulse-height threshold, thereby eliminating smaller pulses. It is expected that by increasing the pulse-height threshold, the number of misclassified pulses will decrease. This statement is supported by results shown in Fig. 9, in which the tail integral A_2 as a function of the total integral A_1 is shown. Both integrals were applied to known pulses. It can clearly be seen in Fig. 9 that the

neutron pulses are very well separated from the point in which the total integral (i.e., pulse height) reaches a high enough value. Thus by increasing the pulse-height threshold, we eliminate the small pulses, which are difficult to classify. On the other hand, such pulse elimination leads to a partial loss of information about the initial neutron spectrum. The importance of the missing information cannot be evaluated a priori because it depends on the type of the initial neutron spectrum and the unfolding technique applied.

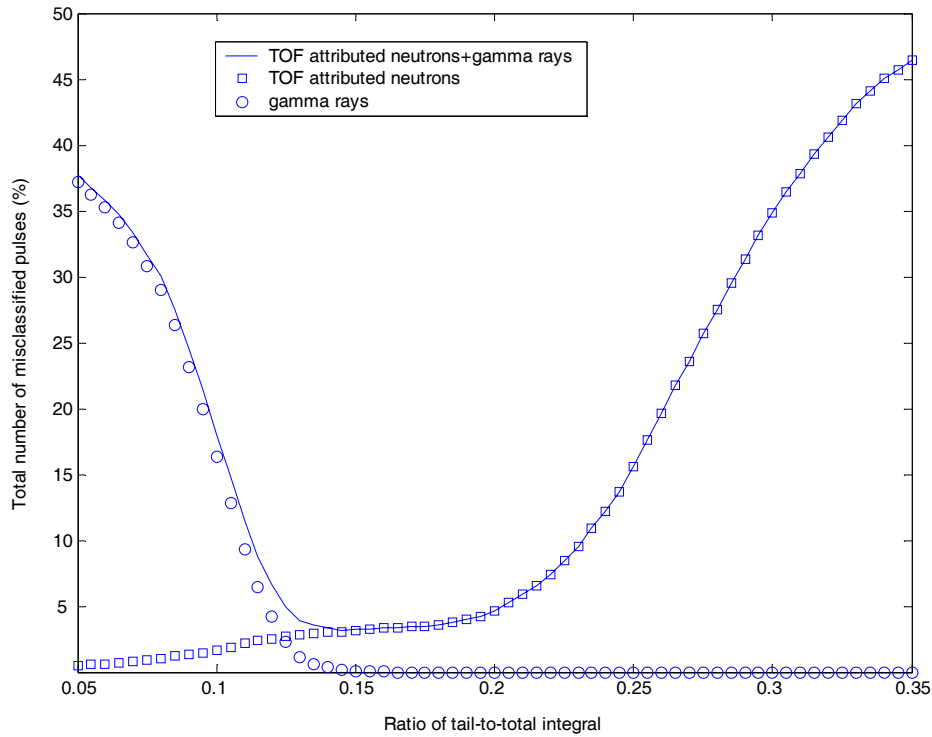


Fig. 8. Total overlap area as a function of the ratio of the tail-to-total integral. The ratio of 0.15 was chosen as the optimal value.

Fig. 9 also shows that some TOF attributed neutron pulses are located in the gamma-ray area. It has been concluded that these pulses were in fact gamma rays that were accidentally identified as neutrons. Fig. 10 shows the case in which the optimized classification threshold ($R=0.15$) was applied to known pulses. The pulses were classified based on their integral ratio R . In this case, most of the incorrectly identified neutrons shown in Fig. 9 were classified as gamma rays.

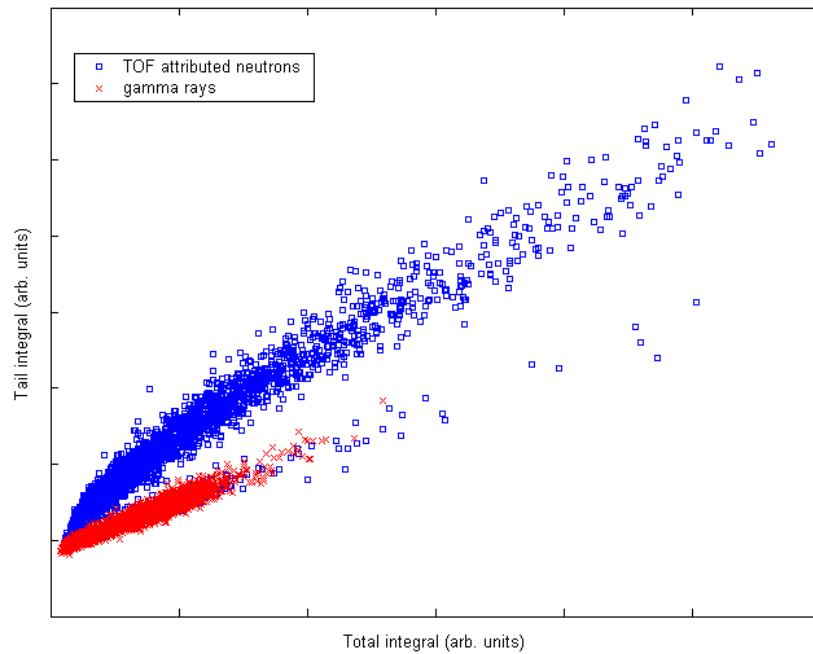


Fig. 9. The tail integral versus the total integral from raw data. Time-of-flight (TOF) attributed neutron and gamma-ray pulses are very well separated. Some pulses attributed as neutrons lie in the gamma-ray area.

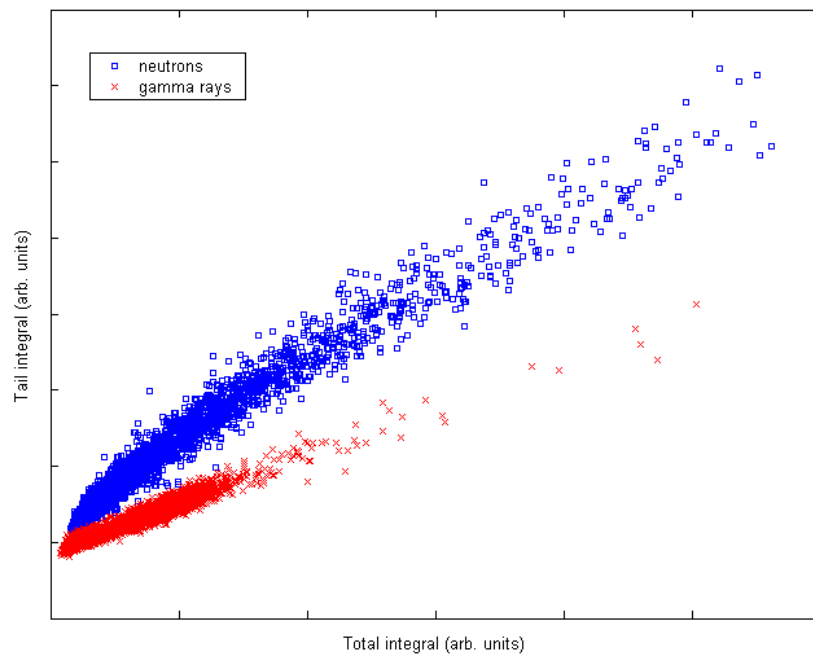


Fig. 10. The tail integral versus the total integral using the optimized pulse-shape discrimination method. Most of the neutron pulses located in the gamma-rays area (see Fig. 9) were identified as gamma rays.

4.3.5 Application of the optimized PSD method to known neutron pulses

Fig. 11 shows the pulse-height curves created from the TOF attributed neutron pulses. Three pulse-height distributions are compared in Fig. 11. They were created from

- (a) TOF attributed neutrons,
- (b) classified neutrons using the optimized PSD method, and
- (c) misclassified neutrons.

It can be concluded from Fig. 11 that most of the neutrons were classified correctly, while only 6% of them were misclassified as gamma rays. The misclassified neutrons are mostly small pulses. As noted in Sect. 4.3.4, many of these neutrons were incorrectly identified gamma rays, and thus the true number of misclassified neutrons is far below 6%. For this reason, the curve “classified neutrons” in Fig. 11 can be considered as a better representation of the neutron source than the curve “TOF attributed neutrons.”

The number of misclassified particles can be further minimized by increasing the pulse-height threshold (see discussion in Sect. 4.3.4). However, this step (if needed) should be performed in close relation to the unfolding technique applied because eliminating pulses below a certain threshold will alter the resulting pulse-height spectrum.

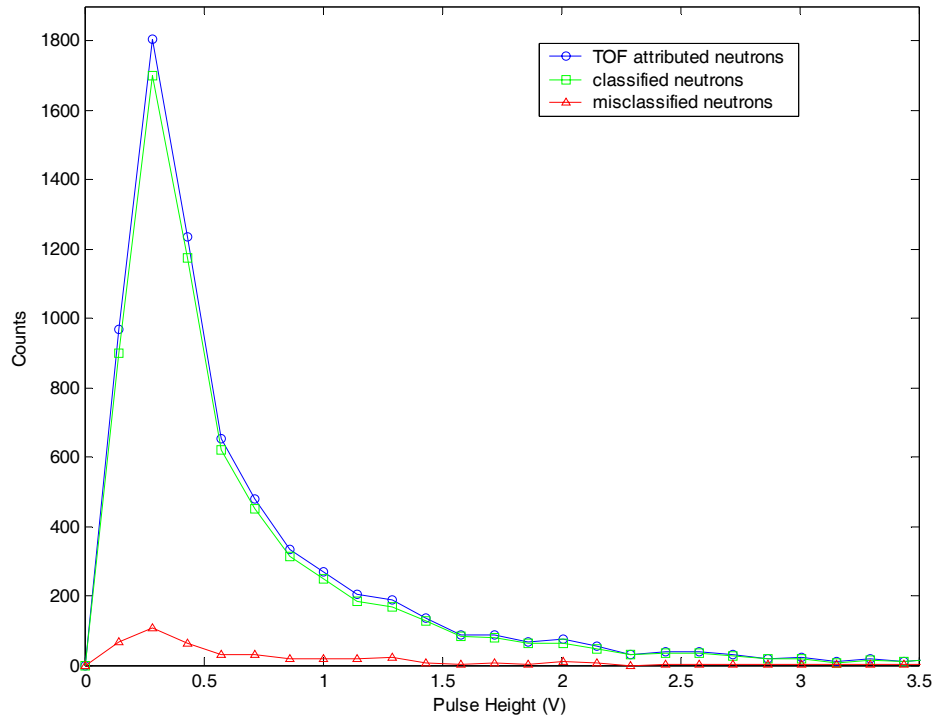


Fig. 11. Comparison of pulse-height distributions created using known neutron pulses.

4.4 Application of the Optimized PSD Method to Unknown Pulses

The digital oscilloscope, scintillation detector, and Cf-252 neutron source described in Sect. 4.1 were used. In the measurement no TOF method was applied, so neutrons could not be directly discriminated from the gamma rays. Instead, the PSD technique discussed earlier was used. Two cases were investigated: the first with no shield between the source and the detector, the second with a lead shield with a thickness of 2.2 cm. Fig. 12 shows a photograph of the measurement setup.

Fig 13 shows the histogram created from the measured data. In the case without shielding, no observable separation of the neutron and gamma-ray distributions occurs. The reason is that the Cf-252 source was placed close to the detector (~ 10 cm), and thus the probability of detecting a neutron simultaneously with some gamma ray was relatively high. It also has to be noted that the condition of the measurement was not the same when compared to that presented in Fig. 7. In particular, the gain of the detector was lower during these measurements. As a result, the lower gain gives rise to the measurement of smaller pulses, which are generally more difficult to identify. In fact, below a certain pulse-height threshold the neutron pulses cannot be discriminated from the gamma-ray pulses. In this case, the pulse-height threshold was set to 0.08 MeVee. The situation can be improved by using the lead shield, as shown in Fig. 13. The shield allowed the relative number of neutron pulses acquired to increase due to elimination of some source gamma rays. Most of these gamma rays possessed low pulse heights (low energy); thus the neutron/gamma discrimination has been improved. However, it is expected that a better discrimination would be achieved by keeping the measurement conditions constant during the PSD optimization and the consequent measurement of unknown pulses, and by increasing the source-detector distance.

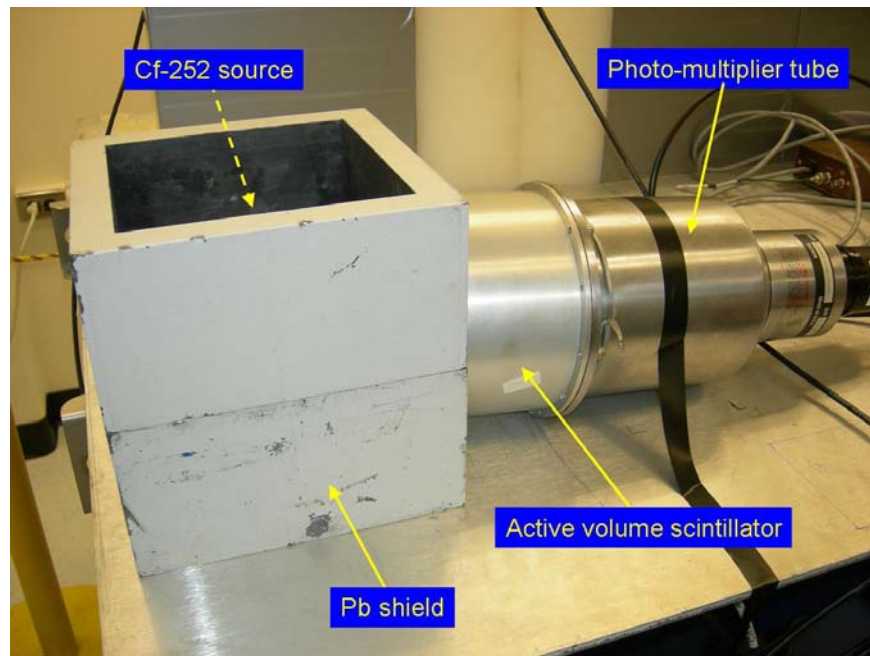


Fig. 12. The measurement setup used to test the optimized pulse-shape discrimination method.

A comparison of pulse-height distributions is shown in Fig. 14. The data were normalized per area. Because the measurement of unknown pulses without the shield cannot be used for the neutron discrimination (see Fig. 13), the measurement with the shield was used instead. The value used as a classification point in the PSD method was deduced from Fig. 13; it is $R = 0.26$. This value is different from the value given in Sect. 4.3.3 ($R = 0.15$) due to different measurement conditions.

A fairly good agreement has been achieved: the position of the peaks is similar in both cases. However, the separation of the neutron and gamma-ray peaks is much worse than in the case of TOF attributed neutrons. We think the PSD can be improved by setting the measurement conditions constant during the PSD optimization and the measurement of pulses. Fig. 14 shows that more low-peak pulses appear in the curve “discriminated neutrons,” which is caused by collisions of detected gamma rays and neutrons with the lead shield. Some of these gamma rays are classified as neutrons, which further deforms the pulse-height curve.

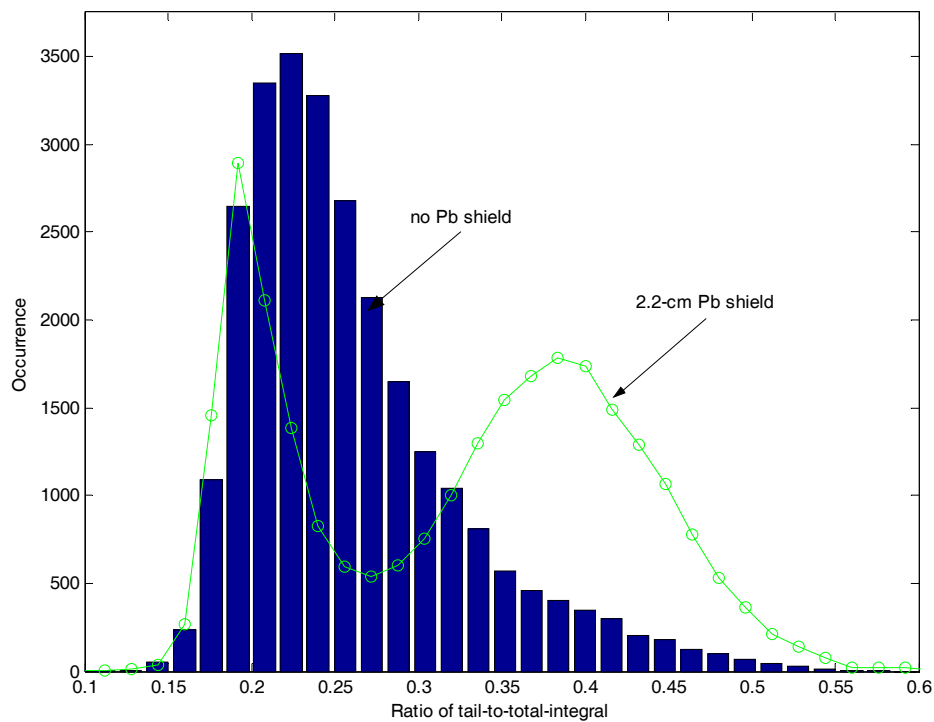


Fig. 13. Histogram from unknown data. The curve shows the improvement in the separation of neutron and gamma-ray pulses when a lead shield is used.

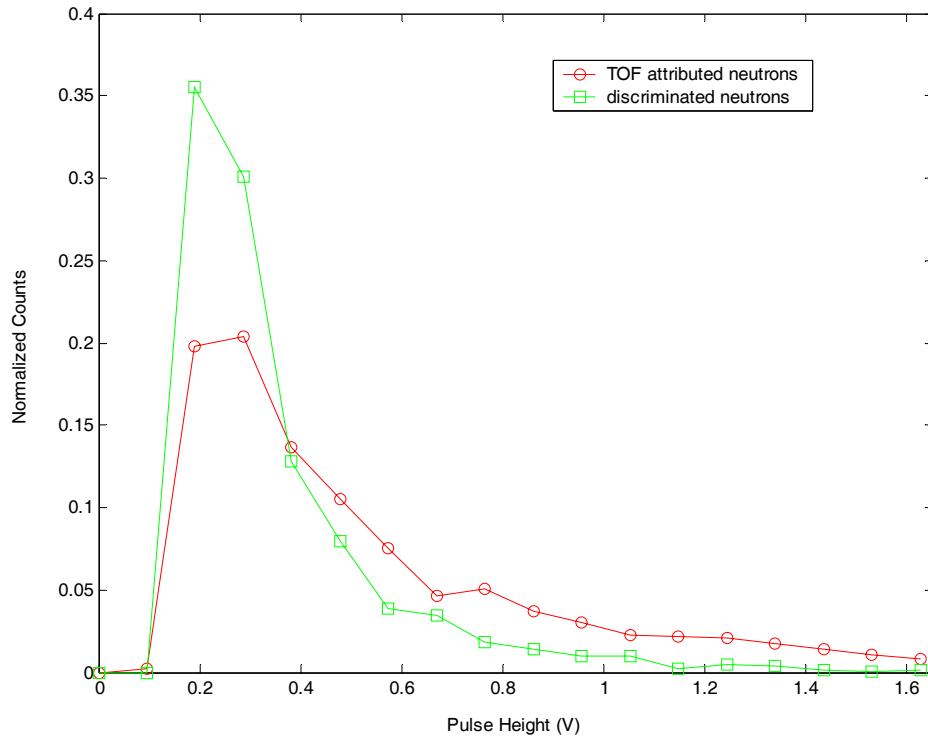


Fig. 14. Comparison of neutron pulse-height distributions; known versus unknown data. The distribution obtained from known neutron pulses is compared with the one obtained using the pulse-shape discriminator method. The lead shield was used to improve the level of the neutron discrimination.

5. Conclusions and Future Work

A PSD technique has been optimized to classify the neutron and gamma-ray pulses measured with a liquid scintillator. This offline method can be used to discriminate neutrons from gamma rays originating from a neutron source with high accuracy. The final optimization has been achieved by combining TOF measurements with Matlab® calculations. A fast oscilloscope Tektronix TDS-5104 was used to store pulses originating from the liquid scintillation detector BC-501A for subsequent analysis. The Matlab® program was used to post-process the pulses measured with the liquid scintillation detector. Following the difference in the slow component of pulses, a specific ratio of tail-to-total integral was proposed for classifying the particles. The integration time was on the order of 130 ns, which is considerably shorter than integration times reported in the literature.

The tail integration range and location of the classification point were optimized using TOF attributed neutron pulses. In this way, the number of misclassified particles was minimized. With the optimized PSD technique we obtained a 3% error in the classification of known pulses with a threshold of 0.07 MeVee. We also conclude from our measurement results that the condition of the measurement during the optimization of the PSD method and subsequent measurement of unknown pulses should be kept constant. In particular, the gain of the detector plays an important

important role. Generally, lower detector gain causes the measured pulses to be smaller and more difficult to classify.

The level of neutron discrimination can be further improved by increasing the pulse-height threshold. On the other hand, this can lead to a certain loss of information about the initial neutron spectrum; therefore, this optimization requires a feedback from the unfolding technique being applied. In particular, the properties of the unfolding technique should determine the maximum allowable pulse height used as a pulse threshold. In this way, additional improvement of the PSD method proposed can be achieved.

New measurements are currently being performed to test and further improve the PSD method. As a next step, other shielding materials will be used to reveal how these materials influence the accuracy in obtaining the initial source spectrum. In addition, similar measurements and Matlab® calculations will be performed using an americium-beryllium neutron source.

6. Acknowledgments

The authors thank Paul Hausladen for interesting discussions on PSD optimization methods. This work was supported by the Oak Ridge National Laboratory and U.S. Department of Energy, National Nuclear Security Administration Office of Nonproliferation Research Engineering (NA-22).

7. References

1. J. A. Mullens, J. D. Edwards, and S. A. Pozzi, "Analysis of Scintillator Pulse-Height for Nuclear Material Identification," Institute of Nuclear Materials Management 45th Annual Meeting, Orlando, Florida, July 18–22, 2004.
2. G. Ranucci, P. Goretti, and P. Lombardi, "Pulse Shape Discrimination of Liquid Scintillators," *Nucl. Instr. Meth. A*, **412**, 374–386 (1998).
3. M. Moszynski et al., "Study of N-Gamma Discrimination with NE213 and BC501A Liquid Scintillators of Different Size," *Nucl. Instr. Meth. A*, **350**, 226–234 (1994).
4. S. D. Jastaniah, P. J. Sellin, "Digital pulse-shape algorithms for scintillation-based neutron detectors," *IEEE Transactions on Nuclear Science*, **49**, 1824–1828 (2002).
5. L. Bertalot et al., "Fast digitizing techniques applied to scintillation detectors," *Nucl. Phys. B*, **150**, 78–81 (2006).
6. S. A. Pozzi and S. Avdic, *Neutron and Gamma-Ray Pulse Shape Data Acquisition from a Cf-252 Source*, ORNL TM-2006/62 (April 2006).
7. L. M. Bollinger and G. E. Thomas, "Measurement of the Time Dependence of Scintillation Intensity by a Delayed-coincidence Method," *Rev. Sci. Instrum.*, **32**, 1044 (1961).

INTERNAL DISTRIBUTION

- | | |
|----------------------|------------------------------|
| 1-2. M. Flaska | 10. J. S. Neal |
| 3. Z. W. Bell | 11-12. S. A. Pozzi |
| 4. C. S. Blessinger | 13. T. Uckan |
| 5. P. A. Hausladen | 14. J. A. Williams |
| 6. J. J. Henkel | 15. M. C. Wright |
| 7. J. A. March-Leuba | 16. Central Research Library |
| 8. J. T. Mihalczo | 17. ORNL Laboratory Records |
| 9. J. A. Mullens | |